Terahertz vibration–rotation–tunneling spectroscopy of water clusters in the translational band region of liquid water

Frank N. Keutsch
Department of Chemistry, University of California Berkeley, Berkeley, California 94720

Mac G. Brown
Department of Chemistry, University of Oregon, Eugene, Oregon 97403

Poul B. Petersen and Richard J. Saykally[a)]
Department of Chemistry, University of California Berkeley, Berkeley, California 94720

Michel Geleijns and Ad van der Avoird
Institute of Theoretical Chemistry, NSR-Center, University of Nijmegen, Toernooiveld, 6525 ED Nijmegen, The Netherlands

(Received 7 July 2000; accepted 10 November 2000)

We report the first direct observation of the hydrogen-bond stretching vibration for a water cluster. A perpendicular band of $(D_2O)_3$ was measured by terahertz laser vibration–rotation–tunneling spectroscopy at 142.8 cm^{-1} in the ''translational band'' region of the liquid corresponding to the hindered translational motions of water molecules. We have tentatively assigned the spectrum to transitions from the vibrational ground state to the degenerate hydrogen-bond stretch or a combination or mixed state of the degenerate stretch and a torsional vibration. Comparison with theoretical results shows that calculated frequencies are much too high, presumably because they do not include coupling between the torsional and stretching vibrations. © *2001 American Institute of Physics.* [DOI: 10.1063/1.1337051]

I. INTRODUCTION

In recent years the study of small water clusters in the gas phase has been stimulated by the prospects for determining an accurate intermolecular potential for water as well as for unraveling the molecular details of the hydrogen-bond dynamics.[1–12] Water clusters have now been studied in great detail by microwave and terahertz laser vibration–rotation–tunneling (THz-VRT) spectroscopy at low frequencies (<105 cm^{-1}), and in less detail in the mid-infrared by a variety of methods including infrared cavity ringdown spectroscopy.[1,7,11,13–16] There have been numerous theoretical efforts comparing the THz-VRT results with calculations employing both *ab initio* results and empirical potentials. The experimental results have allowed the determination of the two most accurate intermolecular water pair potential to date. The first is the VRT(ASP-W) potential of Fellers *et al.*,[12] who made a six-dimensional fit based on Stone's ASP-W potential to water dimer spectroscopic data. This polarizable potential accurately reproduces the experimentally determined properties of the water dimer as well as the second virial coefficients of water and it even reproduces the structures of the trimer and tetramer, since it implicitly contains the dominant many-body interaction (induction). What is missing for describing the bulk phases of water at this point is principally the three-body exchange interaction, which constitutes ~10% of the liquid cohesive energy.[17,18] The second accurate water pair potential is SAPT-5*s*-tuned[19] based on the SAPT-5*s* potential fit to a large number of *ab initio* data points computed by symmetry-adapted perturbation theory (SAPT). This potential was improved by tuning it to spectroscopic data in six-dimensional calculations of the water dimer far-infrared spectrum. When supplemented with explicitly calculated three-body interactions obtained by SAPT, it reproduces not only the equilibrium structure of the water trimer, but also the measured torsional frequencies.

The water trimer, the structure of which is shown in Fig. 1, is thus the key to the next step toward developing an accurate model for the bulk, as the VRT data allow explicit quantification of three-body forces. Current interest in the water trimer is evidenced by the large number of recent theoretical calculations investigating its structure, torsional potential energy surface, vibrations, and hydrogen bond tunneling dynamics.[2,8,20–26] Much effort has been spent in collecting an extensive experimental data set for $(H_2O)_3$, $(D_2O)_3$, and the mixed isotopomers by VRT spectroscopy, with four, seven, and six vibrational bands, respectively, observed to date.[26–30]

All previously reported water cluster VRT spectra, with exception of the 137.7 cm^{-1} $(D_2O)_4$ band, lie in or close to the ''bending band'' of liquid water (~60 cm^{-1}). These VRT results have been primarily limited to torsional motions of the free hydrogens, which are not thought to be a dominant motion in room temperature liquid water because of the small number of single donor–single acceptor molecules in the liquid. Although these VRT spectra have facilitated the development and calibration of various potentials and theoretical models, and have yielded much insight into the nature of hydrogen-bond–tunneling dynamics, it would clearly be

a)Author to whom correspondence should be addressed. Electronic mail: saykally@uclink4.berkeley.edu

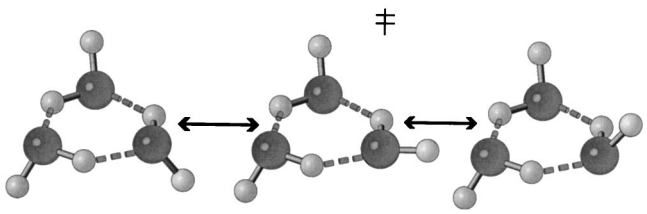

FIG. 1. The equilibrium structure of the water trimer is shown together with one of the two experimentally observed tunneling motions. The facile flipping motion of the free hydrogen/deuterium connects two degenerate minima on the potential energy surface. Altogether six such minima can be interconnected through this torsional motion, splitting each torsional energy level into six.

very interesting to investigate cluster vibrations which more closely resemble those known to occur in liquid water.

The lowest strong vibrational feature of the liquid is the ''translational band,'' centered at 180 cm^{-1} in H_2O and 170 cm^{-1} in D_2O. The hindered translation of water molecules giving rise to this absorption feature is essentially a hydrogen bond stretching vibration, but no detailed experimental study exists that would allow the characterization of these motions on a molecular level. It has been proposed that the hydrogen-bond stretching vibrations in the liquid are local vibrations involving only a very small number of water molecules.[31] The hydrogen-bond stretching vibrations of small water clusters can therefore provide models for translational vibrations in the bulk, especially as the free hydrogens—the main distinction of water clusters from the bulk—are predicted not to influence the stretching vibrations significantly. A study comparing the effect of exciting the various intermolecular vibration on the dynamics of water clusters with liquid water is ongoing. Therefore, we have sought to extend the frequency range of our terahertz spectrometer to enable the study of this novel vibrational motion.

We have investigated the frequency range from 4.1–4.3 THz (137–143 cm^{-1}), thus performing the first high resolution measurements in the translational band region of liquid water. Figure 2 shows the observed transitions for D_2O in relation to the translational band of the liquid. We have assigned a VRT spectrum of $(D_2O)_3$ centered at 4.284 781 79(27) THz to the degenerate hydrogen bond stretch vibration, combination band, or mixed level of the degenerate hydrogen bond stretch and torsional vibrations.

II. EXPERIMENT

The Berkeley terahertz spectrometer used in the observation of the new 142.8 cm^{-1} $(D_2O)_3$ band has been described previously and only the principal features and recent improvements will be discussed here.[32–34] Tunable terahertz laser light is generated by nonlinear mixing of fixed frequency THz radiation with tunable microwave radiation in a Schottky barrier diode. The $9P(34)$ transition of a line tunable CO_2 laser with an output of 85 W is used to pump the 70 μm(4.251 6736 THz)CH_3OH gas laser. The THz radiation and the fundamental, first, or second harmonic of a HP8367B microwave synthesizer (2–26 GHz) are coupled through an antenna onto a 1T24 Schottky barrier diode. Mixing in the diode produces tunable sidebands with frequencies

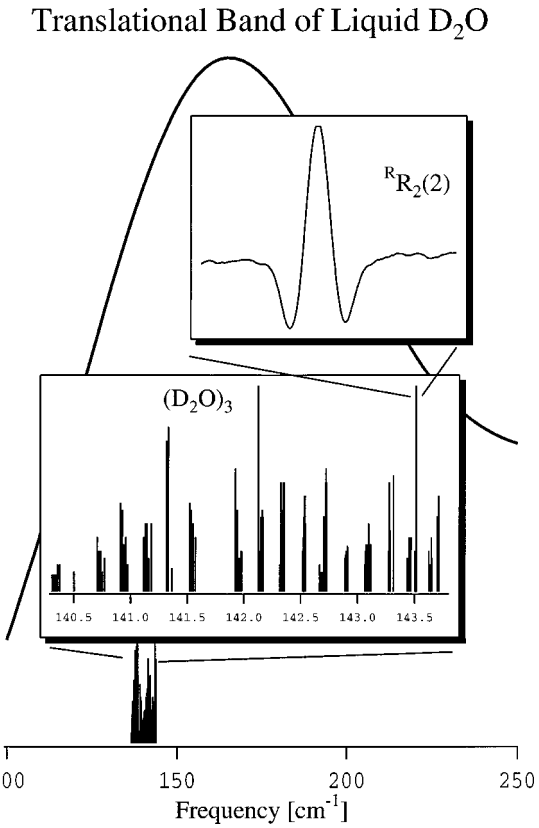

FIG. 2. An overview of the observed D_2O transitions with respect to the translational band of liquid D_2O shows that the 142.8 cm^{-1} band lies well within the translational band of the liquid. The first inset shows a stick spectrum representation of the 142.8 cm^{-1} $(D_2O)_3$ band and the second inset is a scan of the $^{R}R_2(2)$ transition, representative of the strongest observed rovibrational transitions.

of ν(laser)$\pm\nu$(microwave), which results in an effective tuning range of 2–60 GHz centered around each FIR laser. The sidebands are multipassed through a pulsed supersonic expansion of a mixture of argon and D_2O and detected on an unstressed germanium/gallium photoconductive detector. The pulsed molecular beam is produced by expanding pure Ar, saturated with D_2O, through a 101.6 mm-long slit at a repetition rate of 33 Hz while maintaining the vacuum chamber at approximately 35 mTorr with a Roots blower (Edwards EH4200) backed by two rotary pumps (Edwards E2M275).

The extension of the frequency range of our instrument to frequencies larger than 3.0 THz, which corresponds to the translational band region of liquid water, has been made possible through the recent improvements in Schottky barrier technology by Crowe and co-workers.[35] Earlier Schottky barrier diodes designed for high frequency made measurements above 4 THz extremely difficult as the contact between the antenna and the diode was very unstable and it was time consuming to repeatedly reestablish the contact. Although the contact area between the diode and the antenna for the 1T24 diode remains much smaller than the 1T12 Schottky barrier diode used in previous, lower frequency experiments, the stability and time for recontacting are comparable.

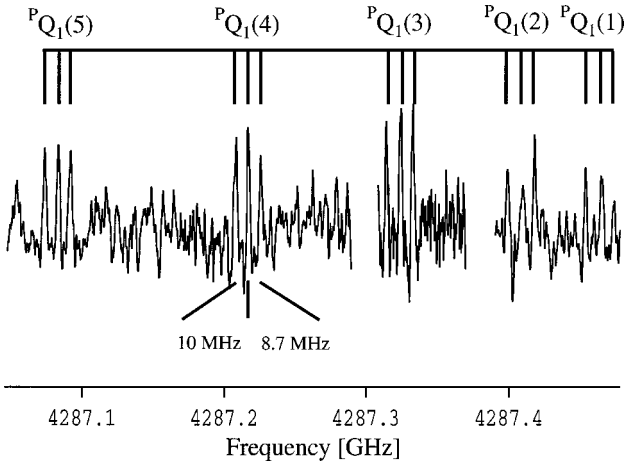

FIG. 3. Inspection of the $^{P}Q_1$-branch shows that all $K=0<-1$ transitions are split into equal intensity triplets within the experimental uncertainty. The spacing is about 10 and 8.7 MHz.

III. RESULTS

We report the observation of an *a*-type VRT spectrum of $(D_2O)_3$ at 142.8 cm^{-1} (4.284 781 79(27) THz). As the experimental *A* and *B* rotational constants are identical for the water trimer, *a*-type and *b*-type spectra are identical. A total of 119 transitions were measured with a precision of 3 MHz and assigned by first identifying the *Q*-branches and then using known vibrational ground state combination differences of $(D_2O)_3$ to assign the *P*- and *R*-branch lines. Using combination differences of the first degenerate excited levels resulted in much larger differences between calculated and observed values.

A stick spectrum representation of the new band, together with the observed $^{R}R_2(2)$ transition is shown in the inset of Fig. 2 and is typical for a perpendicular band of an oblate symmetric top. The most intense transitions were observed in the *R*-branch and have a signal-to-noise ratio (S/N) of about 30:1. This can be compared to a S/N ratio of about 8000:1 for the strongest torsional band (sum of all bifurcation tunneling components). The linewidths were about 3.7 MHz slightly larger than the Doppler limited linewidths observed in the 4.1 THz(137.7 cm^{-1})$(D_2O)_4$ band. Bifurcation tunneling splittings were not observed, in contrast to all previously observed $(D_2O)_3$ bands except for the 583.2 GHz band reported in the previous paper. Decreasing the modulation depth revealed barely observable shoulders on each line, indicating possible bifurcation tunneling splittings of less than 1 MHz. Due to the decrease in signal intensity accompanying reduced modulation depth this was only observable for the strongest transitions. No *R*-branch transitions higher in frequency than $^{R}R_3(3)$ were observable due to limitations of the microwave frequency available for sideband generation.

The spectrum exhibits severe Coriolis perturbations. Compared to other *Q*-branches, the $^{R}Q_0$-branch is expanded and the $^{P}Q_1$-branch is compressed. The $K'=1$ states of the $\Delta K=+1$ band are split into a doublet, with the $^{R}Q_0$-transitions terminating in the lower energy doublet component and the $^{R}P_0$- and $^{R}R_0$-transitions in the higher energy one. All $K=0<-1$ transitions are split into nearly equally spaced equal intensity triplets, which is readily observable in the $^{P}Q_1$-branch shown in Fig. 3, but is also found for the $^{P}P_1$-branch transitions. The spacing shows no significant dependence on *J*, although there might be a slight decrease of the magnitude of the splitting for higher *J*-values. The spacing of these triplets is nearly equal with about 10.0 and 8.7 MHz (Fig. 3).

Previous work on the torsional states of the water trimer introduced a quantum number *k* associated with the pseudorotational symmetry associated with these states. In the G_6PI group of the water trimer there exist six symmetries and their correlation to the *k*-label are shown in Table I. Selection rules require that the excited state have $k=\pm 2$ symmetry for an *a*-type band originating in the vibrational ground state. The appearance of the spectrum is very similar to that of the 28 and 81.8 cm^{-1} bands of $(D_2O)_3$. Accordingly, the assigned transitions were fit to the energy expression developed for those bands.[26] The assigned transition frequencies are given in Table II together with the differences between observed and calculated frequencies.

The molecular constants determined from this fit are given in Table III. It was not possible to fit the *C*-rotational constants for the excited and the ground state without correlation, and only ΔC will be discussed. The rms deviation of the fit was 0.86 MHz, which is better than the frequency accuracy of the experiment, and the quality of this fit is one of the best obtained for any VRT band measured to date.

TABLE I. Correlation of the pseudorotational quantum number *k* and the symmetry labels in the G_6 group of the water trimer.[a]

Symmetry in G_6	*k*
A_1^+	0
A_3^-, A_2^-	±1
A_3^+, A_2^+	±2
A_1^-	3

[a]From Viant *et al.* (Ref. 26).

IV. VIBRATIONAL ASSIGNMENT AND ANALYSIS

Before discussing the vibrational assignment it is helpful to review some of the characteristics of the previously observed $(D_2O)_3$ bands, insofar as they pertain to the analysis of the band reported here.

A. Previously observed $(D_2O)_3$ bands

Six VRT bands of $(D_2O)_3$ have previously been measured, all of which arise from torsional vibrations and occur at frequencies below 100 cm^{-1}.[26,28] This collection of bands at low frequencies has been explained in detail previously[26] and is caused by the very facile flipping motion of the free deuterons (Fig. 1). Flipping of one of the two free deuterons which are on the same side of the oxygen framework is symmetrically equivalent to a rotation around the figure (c) axis. The barrier for this motion is very near to the zero point energy, giving rise to a very large tunneling splitting and generating the pseudorotational manifold of energy levels shown together with the previously observed transitions between them in Fig. 1 of the preceding paper.[8,25,28] The mo-

TABLE II. The assigned transitions are shown together with the difference between calculated and observed frequencies. The centers of the $K=0<-1$ triplets were used in the fit. The two degenerate vibrational levels are labeled $\nu'=1, 2$, with the level pushed to higher energy by the Coriolis interaction being $\nu'=2$. Label 1 refers to all observed K-values for $\nu'=1$, including the lower of the split $K=1$ states, and label 2 refers to the other $K=1$ state of $\nu'=1$. Label 3 corresponds to K values with $K=J, J-1$ of $\nu'=2$ and label 4 to all other K-values.

ν'	Label	J'	K'	ν''	J''	K''	Frequency (MHz)	Obs.−Calc. (MHz)	ν'	Label	J'	K'	ν''	J''	K''	Frequency (MHz)	Obs.−Calc. (MHz)
1	1	8	5	0	8	4	4258 811.88	−1.35	2	4	5	1	0	5	2	4292 666.64	0.88
1	1	7	5	0	7	4	4259 032.56	0.93	2	4	4	1	0	4	2	4292 804.28	0.82
1	1	6	5	0	6	4	4259 221.44	−0.48	2	4	3	1	0	3	2	4292 914.98	0.14
1	1	5	5	0	5	4	4259 384.28	−0.14	2	3	2	1	0	2	2	4293 000.84	1.75
1	1	9	4	0	9	3	4264 049	0.29	2	4	6	2	0	6	3	4298 105.4	−0.1
1	1	8	4	0	8	3	4264 302.88	0.87	2	4	5	2	0	5	3	4298 270.04	−1.92
1	1	7	4	0	7	3	4264 525.72	0.26	2	4	4	2	0	4	3	4298 413.68	1.66
1	1	6	4	0	6	3	4264 719.52	−0.13	2	3	3	2	0	3	3	4298 526.36	1.42
1	1	5	4	0	5	3	4264 885.84	0.73	2	4	9	3	0	9	4	4303 065.64	−1.42
1	1	4	4	0	4	3	4265 022.5	0.2	2	4	8	3	0	8	4	4303 313.28	0.67
1	1	9	3	0	9	2	4269 539.1	0.43	2	4	7	3	0	7	4	4303 532.76	−0.75
1	1	8	3	0	8	2	4269 800.4	−1.33	2	4	6	3	0	6	4	4303 727.52	−1.32
1	1	7	3	0	7	2	4270 032.2	−0.34	2	4	5	3	0	5	4	4303 897.8	0.03
1	1	6	3	0	6	2	4270 232.7	0.55	2	3	4	3	0	4	4	4304 038.8	−0.82
1	1	5	3	0	5	2	4270 402.5	1	2	4	9	4	0	9	5	4308 699.6	0.17
1	1	4	3	0	4	2	4270 542.3	0.91	2	4	8	4	0	8	5	4308 948.84	−0.45
1	1	3	3	0	3	2	4270 652.3	−0.19	2	4	7	4	0	7	5	4309 173.72	0.1
1	1	7	2	0	7	1	4275 541.92	−0.05	2	4	6	4	0	6	5	4309 370.88	−0.76
1	1	6	2	0	6	1	4275 753	−0.49	2	3	5	4	0	5	5	4309 542.84	0.19
1	1	5	2	0	5	1	4275 930.12	−0.68	2	3	1	0	0	2	1	4264 277.92	0.09
1	1	4	2	0	4	1	4276 076.24	0.52	2	4	3	0	0	4	1	4240 960.48	0.26
1	1	3	2	0	3	1	4276 189.92	0.12	2	4	4	0	0	5	1	4229 266.72	0.75
1	1	2	2	0	2	1	4276 273.32	−0.95	2	3	1	1	0	2	2	4269 868.76	−1.76
1	1	8	1	0	8	0	4279 997.4	0.98	2	3	2	1	0	3	2	4258 223.28	0.05
1	1	7	1	0	7	0	4280 420.3	−0.97	2	4	3	1	0	4	2	4246 550.28	−0.01
1	1	6	1	0	6	0	4280 793.4	−0.34	2	4	4	1	0	5	2	4234 854.4	1.37
1	1	5	1	0	5	0	4281 113.3	−0.25	2	4	5	1	0	6	2	4223 132.76	−0.2
1	1	4	1	0	4	0	4281 379.5	−0.93	2	3	2	2	0	3	3	4263 831.44	−1.65
1	1	3	1	0	3	0	4281 594.8	0.61	2	4	4	2	0	5	3	4240 458.97	−0.63
1	1	2	1	0	2	0	4281 754.8	0.14	2	4	5	2	0	6	3	4228 737.36	0.6
1	1	1	1	0	1	0	4281 861.5	−0.21	2	3	3	3	0	4	4	4257 786.48	1.07
1	2	2	1	0	1	0	4305 091.56	−1.21	2	3	4	3	0	5	4	4246 083.96	−0.43
1	2	1	1	0	2	0	4258 728.12	−0.38	2	4	5	3	0	6	4	4234 359.52	0.31
1	2	2	1	0	3	0	4247 133.8	0.37	2	4	6	3	0	7	4	4222 608.7	−2.44
1	2	3	1	0	4	0	4235 536.08	−2.19	2	4	7	3	0	8	4	4210 840.2	−1.38
1	1	2	2	0	1	1	4299 457.6	−1.26	2	3	5	4	0	6	5	4240 000.04	0.27
1	1	3	2	0	2	1	4310 964.84	−0.1	2	4	6	4	0	7	5	4288 249.68	0.78
1	1	3	3	0	2	2	4305 427.8	−0.55	2	3	5	5	0	6	6	4245 658.82	0.53
1	1	4	4	0	3	3	4311 388.8	0.36	2	3	6	5	0	7	6	4233 905.8	1.16
2	4	7	0	0	7	1	4286 752.24	0.78	2	4	7	5	0	8	6	4222 129.44	1.05
2	4	6	0	0	6	1	4286 927.48	0.52	2	4	8	5	0	9	6	4210 330.3	−0.55
2	4	5	0	0	5	1	4287 082.52	0.24	2	3	6	6	0	7	7	4239 578.4	0.23
2	4	4	0	0	4	1	4287 215.48	0.29	2	3	7	6	0	8	7	4227 799.6	0.97
2	4	3	0	0	3	1	4287 324.32	0.52	2	3	7	7	0	8	8	4233 485.3	−1.11
2	4	2	0	0	2	1	4287 407.24	0.65	2	3	8	7	0	9	8	4221 682	0.72
2	3	1	0	0	1	1	4287 463.04	0.62	2	4	9	7	0	10	8	4209 855.1	−0.11
2	4	9	1	0	9	2	4291 876.8	1.48	2	3	8	8	0	9	9	4227 381.7	−0.78
2	4	8	1	0	8	2	4292 105.04	−1	2	3	9	9	0	10	10	4221 265.4	−0.39
2	4	7	1	0	7	2	4292 316.24	0.5	2	3	10	9	0	11	10	4209 411.1	0.68
2	4	6	1	0	6	2	4292 503.68	0.9									

lecular constants describing the torsional energy levels, together with some characteristics of the observed bands are in Tables IV and V.

All bands involving degenerate levels are perturbed, and both the 28 and 81.8 cm^{-1} bands show splittings of the $K=1$ level of the $\Delta K=+1$ transitions and have anomalous bifurcation tunneling splittings of the $K=0<-1$ transitions. The perturbation is of the form expected for first-order Coriolis interactions with K-type doubling. van der Avoird *et al.*'s detailed treatment of the water trimer including the torsional and bifurcation tunneling motion as well as overall rotation showed that while the flipping motion is symmetrically equivalent to rotation around the C-axis, the expectation value for first-order vibrational angular momentum is zero and there can therefore be no first-order Coriolis interaction.[25,36] The recent fits of all previously observed $(D_2O)_3$ bands to van der Avoird *et al.*'s model explains nearly all observed perturbations for these bands.[26,28]

TABLE III. The molecular constants determined for the 142.8 cm^{-1} $(D_2O)_3$ band are shown. All values are in MHz except for ζ which is dimensionless. Only ΔC was determined as it was not possible to fit C' and C'' without correlation. $\Delta\Delta = \Delta B - 2\Delta C$ is related to the difference in inertial defect, $\Delta(\Delta = I_c - I_a - I_b)$, between the excited state and ground state. Like the inertial defect, it is a measure of planarity of a molecule, with a planar molecule having $B - 2C = 0$, and $\Delta = 0$, and a negative sign indicates nonplanarity. ζ is the linear Coriolis term and $|\mu_{++}|$ the second order term developed by Viant and Geleijns.[a] The excited state of the 142.8 cm^{-1} band is the first $(D_2O)_3$ or $(H_2O)_3$ band with a negative ΔC and has the smallest increase of the inertial defect for any band.

	Ground State[b]	Excited States[b]	
E_0	0.0	4284 781.9(3)	
$B(=A)$	5796.34(5)	5782.33(5)	
ΔC	0[c]	−5.03(6)	
D_J	0.0292(8)	0.0274(8)	0.0280(7)
D_{JK}	−0.040(3)	−0.045(3)	−0.038(4)
D_K	0.0084(47)	0.011(3)	0.011(6)
ζ[a]	0.0	−0.02708(2)	
$\lvert\mu_{++}\rvert$[a]	0.0	12.81(2)	
$\Delta\Delta$	0.0	−3.95	

[a]As defined by Viant *et al.* (Ref. 26).
[b]1σ uncertainties of fitted constants in parenthesis.
[c]Fixed.

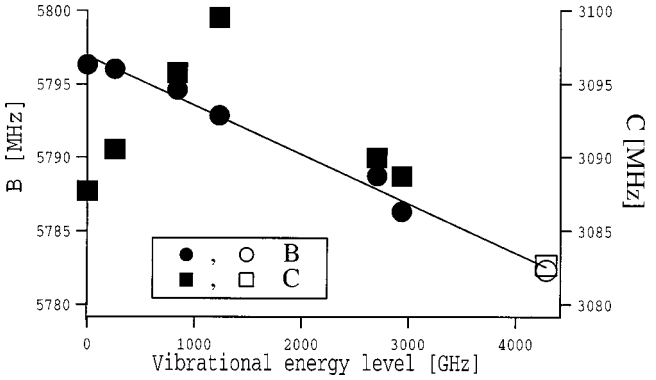

FIG. 4. Experimental values of the *B* and *C* rotational constants vs. vibrational energy (Ref. 26). The closed circles and squares, respectively, correspond to the *B*- and *C*-values for the previously observed torsional bands and the open circle and square correspond to the *B*- and *C*-value of the 142.8 cm^{-1} band presented here. Also shown is a linear fit of the values of the previously observed *B*-rotational constants vs. vibrational energy.

The *B* rotational constant decreases with increasing torsional energy, whereas the *C*-rotational constant is larger for all excited torsional energy levels than for the ground state (see Fig. 4). This leads to a more negative inertial defect in the excited states, consistent with an out-of-plane torsional vibration. The Coriolis constant appears to decrease for the higher lying torsional manifold $(k \pm n^1)$ and ζ is already close to zero in the $\pm 2^1$ level.

All previously observed $(D_2O)_3$ bands share a distinctive feature in that each transition is split into an equally spaced quartet with a characteristic intensity pattern. This splitting arises from the bifurcation tunneling motion, which connects eight degenerate minima on the potential energy surface requiring an expansion of the PI Group from G_6 to G_{48}. The tunneling motion splits each symmetry in the G_6 group into four states (e.g., $A_2^+ \Rightarrow A_{2g}^+, T_u^+, T_g^+, A_{2u}^+$) with characteristic nuclear spin weights of ~7:11:5:1, which is reflected in the observed intensity pattern. The magnitude of the tunneling splitting increases with the energy of the vibrational level whereas the observed splittings do not follow a smooth trend, as they can arise either from the difference or the sum of the bifurcation tunneling splittings in the ground and excited state (see Table V). The bifurcation–tunneling motion consists of the exchange of a bound and a free deuterium atoms of one water molecule accompanied by an odd number of flips of neighboring water molecules. This weak coupling between the torsional motion (flip) and the bifurcation tunneling pathway probably explains the slight increase in the magnitude of the splitting with increasing torsional energy.

Both the 28 and 81.8 cm^{-1} bands have anomalous bifurcation tunneling splittings in the $K = 0 < -1$ transitions. In the degenerate vibrational levels there exist two degenerate T_g- and T_u-states, whereas the *A*-states are nondegenerate. The two degenerate *T*-states are connected via the bifurcation–tunneling pathway and split, resulting in four states, which together with the *A*-states gives rise to six tunneling components. The magnitude of the tunneling splittings is such that a pseudoquartet appears again, but with an unusual intensity ratio of 248:54:108:70 (see Fig. 5). The magnitude of the observed splitting for this pseudoquartet is very similar to the regular bifurcation tunneling splitting. This is only observed for the $K = 0$ levels, as the other levels are not degenerate because their splitting is proportional to *K* via the Coriolis interaction.[25,36]

TABLE IV. The molecular constants of all previously observed $(D_2O)_3$ torsional levels are shown.[c] All values are in MHz, except for ζ which is dimensionless. ΔC is positive and $\Delta\Delta$ negative for all torsional states. ζ is nearly negligible for the higher torsional states.

(k,n)	$0^{0\,a}$	$+1^{0\,a}$	$-1^{0\,a}$	$+2^{0\,a}$	$-2^{0\,a}$	$3^{0\,a}$	$3^{1\,a}$	$+2^{1\,a}$	$-2^{1\,a}$
E_0	0.0[b]	255 976.49(4)		839 186.81(3)		1232 139.43(4)	2709 548.14(6)	2940 936.95(4)	
$B(=A)$	5796.34(2)	5796.04(3)		5794.64(3)		5792.87(3)	5788.73(3)	5786.32(2)	
ΔC	0.0[b]	2.84(5)		8.08(3)		11.83(2)	2.26(5)	0.99(2)	
D_J	0.0293(3)	0.0297(4)	0.0288(4)	0.0271(4)	0.0261(4)	0.0265(5)	0.0286(5)	0.0278(4)	0.0285(4)
D_{JK}	−0.042(1)	−0.050(1)	−0.050(1)	−0.044(1)	−0.039(2)	−0.045(1)	−0.044(1)	−0.048(1)	−0.041(1)
D_K	0.016(2)	0.023(2)	0.028(3)	0.020(2)	0.016(3)	0.022(2)	0.021(2)	0.027(3)	0.014(1)
ζ[c]	0.0	−0.04387(2)		−0.04819(2)		0.0	0.0	0.00031(2)	
$\lvert\mu^{++}\rvert$[c]	0.0	26.68(1)		13.67(3)		0.0	0.0	3.61(1)	
$\Delta\Delta$	0	−5.98		−17.86		−27.13	−12.13	−12	

[a]1σ uncertainties of fitted constants in parenthesis.
[b]Fixed.
[c]Results from Viant *et al.* (Ref. 26).

TABLE V. The magnitude of the bifurcation tunneling splitting increases with torsional energy. The calculated and experimental relative intensities of all previously observed (D_2O_3) vibrational bands from the vibrational ground state are comparable. The experimental relative intensity of the 98.1 cm^{-1} band is smaller than the calculated one as it was scanned with an older source generation. In contrast the bifurcation tunneling splitting of the 142.8 cm^{-1} band is close to that of the vibrational ground state and the intensity is dramatically smaller than that calculated for the next allowed torsional transition ($\pm 2^2 < -0^0$).

Frequency (cm^{-1})	Assignment	Bifurcation–Tunneling Splitting [MHz]	Relative Intensities	
			Experimental	Calculated[f]
19.5[a]	$\pm 2^0 < -\pm 1^0$	<1		
28.0[b]	$\pm 2^0 < -0^0$	0.9	5.0	11
41.1[c]	$\pm 3^0 < -0^0$	1.5	125.0	125
81.8[b]	$\pm 3^1 < -\pm 1^0$	2.7		
89.6[d]	$\pm 2^1 < -\pm 1^0$	5		
98.1[e]	$\pm 2^1 < -0^0$	5	5.0	35
166.7[f]	$\pm 2^2 < -0^0$	~10		11
142.8[g]		<1	0.6	

[a]Results by Keutsch *et al.* (Ref. 28).
[b]Results by Viant *et al.* (Ref. 26).
[c]Results by Suzuki *et al.* (Ref. 1).
[d]Results by Pugliano *et al.* (Ref. 39).
[e]Results by Olthof *et al.* (Ref. 36).
[f]Results by Geleijns *et al.* (Refs. 37, 38).
[g]Reported here.

B. Vibrational assignment

Ab initio calculations predict a number of states between 100 and 200 cm^{-1} with the observed excited state symmetry.[5] The first is the lowest heretofore unobserved purely torsional energy level of A_3^+ ,A_2^+ symmetry, which we will call $\pm 2^2$, calculated to lie at 167 cm^{-1}.[36] Although this energy is about 15% too high, it is not unreasonable as the calculated value for the torsional energy level at 98 cm^{-1} is also 10% too high. According to Sabo *et al.*, the $\pm 2^2$ level may well consist of a combination level of the τ_1 and τ_2 torsional modes, whereas all previously observed levels only involve the τ_1 normal mode.[8] Of course, a normal mode description is poor for large amplitude motions and every vibration can certainly be a combination of the normal mode motions.

All other calculated levels involve the hydrogen-bond stretching vibrations. *Ab initio* calculations generally give three stretching vibrational frequencies: the symmetric stretch at about 175–210 cm^{-1}, and two asymmetric-stretch frequencies at somewhat lower frequency.[3,5] The symmetric stretch has A_1^+ symmetry and could therefore only be observed in a combination band with the $\pm 2^0$ torsional level. It is unlikely that the 142.8 cm^{-1} band corresponds to this case, as the intensity of such a combination band would be extremely weak.[5] Furthermore, the estimate of the symmetric stretch frequency is probably better than for the case of both the very anharmonic torsions and the asymmetric stretch as this is expected to couple strongly to the torsions, which would lead us to expect such a combination band of symmetric stretch and torsion at much higher energies. The situation for the asymmetric stretch is more complicated. The ground state wave function of $(D_2O)_3$ is equivalent to that of an oblate symmetric top, and thus one expects a degenerate asymmetric hydrogen-bond stretching vibration of the observed symmetry rather than two distinct asymmetric vibrations.[21] This degenerate asymmetric stretch itself also is of $k=\pm 2$ symmetry and could therefore correspond to the observed band. Sabo *et al.* point out that the degenerate

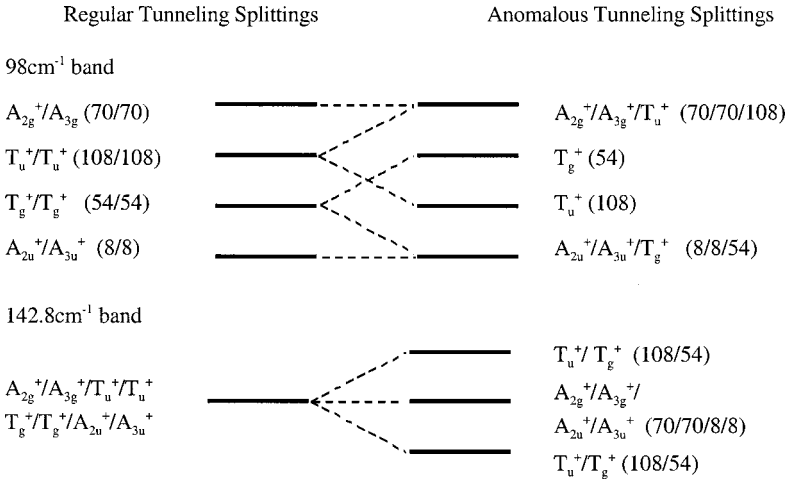

FIG. 5. Anomalous bifurcation tunneling splittings of the $K=0<-1$ transitions in the 98 and 142.8 cm^{-1} bands (Refs. 25, 36). The splitting of the degenerate *T*-states for $K=0$ of the degenerate vibrations results in a pseudoquartet with an unusual intensity ratio of 248:45:108:70. The magnitude of the observed splitting is nearly identical to that observed for all other *K*-values. Splitting of the degenerate *T*-states for $K=0$ in the 142.8 cm^{-1} band would produce the observed equal intensity triplets if the magnitude of this splitting is about one order-of-magnitude larger than in the regular bifurcation tunneling splittings of all other *K*-values.

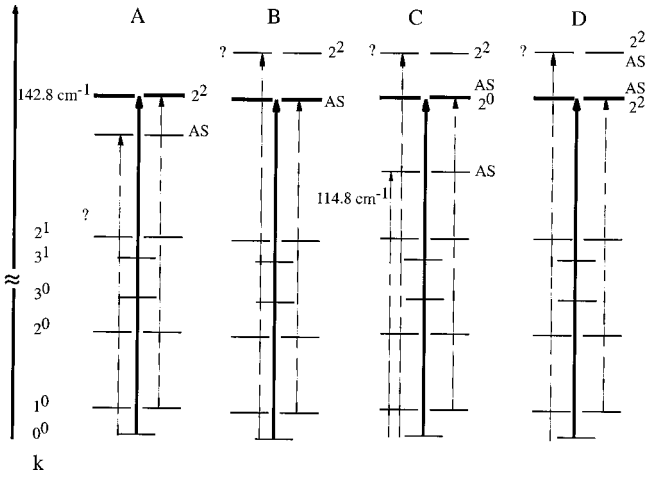

FIG. 6. The four possible vibrational assignments of the 142.8 cm^{-1} band. The 142.8 cm^{-1} band is shown as solid arrow and predicted bands are depicted as dashed arrows. The degenerate asymmetric stretch is labeled AS. **A** corresponds to the case of a purely torsional vibration ($\pm 2^2$), **B** a purely translational vibration (AS), **C** a combination band of AS and the $k=\pm 2^2$ level, and **D** a mixed level of translation and torsion. Analysis of the band intensity, the molecular constants, and the bifurcation tunneling splitting determined for the excited state, indicate that cases **B** and **D** are most likely. A distinction between the latter cases requires a detailed experimental investigation in the 3–5 THz range.

asymmetric stretch could itself give rise to a manifold of pseudorotational energy levels similar to that of the torsional motion, thereby lowering the energy of the first degenerate stretching vibration considerably, as in the case of the torsions.[21] It is also expected that the degenerate asymmetric stretching vibration will generate first-order vibrational angular momentum and furthermore couple strongly to the higher torsional manifolds, allowing combination bands and possibly resulting in mixed modes containing both torsional and stretching motions.[21] Thus there exist three other (in addition to the $k=\pm 2^2$ level) low-lying states with the correct symmetry (see Fig. 6). The first state consists of the pure degenerate asymmetric stretching vibration. The second possible state consists of a combination band of the $\pm 2^0$ torsional mode with the degenerate asymmetric stretch, and the third is a mixed mode involving both the degenerate asymmetric stretch and some excited torsional motion.

A distinction between the four possible assignments, especially the latter three, is only possible through the detailed analysis of the observed molecular constants, perturbations, and intensity of the band.

C. Analysis of 142.8 cm^{-1} band

The similarities between the new band and the 28 and 81.8 cm^{-1} bands, and especially the fact that it was only possible to get a fit of the data using the Hamiltonian developed explicitly for the torsional energy levels, suggests that the vibration at least partially involves a torsional motion. However it should be pointed out, that the excited state of the asymmetric stretch can be viewed as ''combination level'' with the torsional ground state level ($k=\pm 0^0$). This state is already delocalized over the whole torsional subspace and thus even the excited state of the asymmetric stretch corresponds to a $k=\pm 2$ level with large torsional contributions in agreement with the results from the fit.

1. Intensity

The calculated and experimental intensities for all $(D_2O)_3$ bands originating from the ground state are shown in Table V. The intensities of bands originating in the $\pm 1^0$ level are not comparable, as this level is significantly less populated in a supersonic jet than is the ground state. The calculated and experimental relative intensities of the $k=\pm 2^0 \leftarrow -0^0$ and the $k=\pm 3^0 \leftarrow -0^0$ transitions compare fairly well, whereas the experimental intensity of the $k=\pm 2^1 \leftarrow -0^0$ transition is too low, which is due to the fact that it was measured with an older source generation. The largest S/N ratio for a single tunneling component of the $k=\pm 2^0 \leftarrow -0^0$ transitions was about 100:1, corresponding to a S/N ratio of about 250:1 for the sum of all four tunneling components.[26] This is about one order-of-magnitude stronger than observed for the new band, revealing the latter to be the weakest $(D_2O)_3$ spectrum, and indeed one of the weakest water cluster absorptions detected to date. The sensitivity of our spectrometer is comparable at the higher frequencies and we were able to observe transitions from *J*-values as high as 40 for the *R*-branch transitions of the 137.7 $cm^{-1}(D_2O)_4$ band. Table V also shows the calculated intensity for the $k=\pm 2^2 \leftarrow -0^0$ trimer transition, which is comparable to that of the $k=\pm 2^0 \leftarrow -0^0$ transition.[37,38] The low observed intensity of the present VRT band differs significantly from this trend and reflects what might be expected for the pure asymmetric stretch, a mixed asymmetric stretch/torsional vibration, or for a combination band of asymmetric stretch and torsion. The intensity for a combination band is expected to be very small making experimental observation of such a band quite unlikely, and although we cannot rule out this possibility with certainty, no combination band has been observed for any water cluster to date.

2. Molecular constants

Viant *et al.* showed that the experimental value of the *B*-rotational constant of $(D_2O)_3$ decreases linearly with torsional energy and the *B*-value for the 142.8 cm^{-1} band fits this trend quite well (see Fig. 4).[26] This increase was explained with an increase in the average O–O distance by coupling of the symmetric stretch with the torsional motion. Sabo *et al.* have proposed that for the higher torsional levels additional coupling to the degenerate asymmetric stretch is required to rationalize the observed *B*-value.[21] The *C*-rotational constant cannot be determined for the torsional states as it is contaminated by the Coriolis perturbation. These examples show that care has to be taken when extracting a structural interpretation from rotational constants. However it is interesting to attempt such an interpretation as it can reveal information about the nuclear motions of a vibrational state. The 142.8 cm^{-1} band is the only $(D_2O)_3$ or $(H_2O)_3$ band to date that shows a negative value for ΔC. In fact, two times ΔC is close to the value of ΔB, showing that the inertial defect does not increase significantly in the excited vibrational state. This is the smallest increase in inertial

defect of all observed $(D_2O)_3$ bands, far smaller than for the other levels lying at high energy. As the magnitude of the inertial defect correlates with the amount of out-of-plane torsional motion, the most obvious interpretation is that the small change in inertial defect emanates from a small degree of torsion. At the same time, the overall decrease of the rotational constants strongly suggests a stretching motion. Sabo *et al.* have shown that the interpretation of the rotational constants of the torsional energy levels is not straightforward.[21] The vibrational wave function is delocalized over the entire torsional subspace for $(H_2O)_3$ and to a smaller extent for $(D_2O)_3$. It is necessary to look at the nodes or maxima of the torsional wave functions to deduce the structures where the highest probability is located, and then to infer the effect on the rotational constants. Sabo *et al.* have shown that larger torsional excitation does not simply give higher probabilities at larger distances from the plane of the oxygen atoms.[8,21] The calculations for the lower levels show an increase of the *C*-constant with energy within each manifold, with a sudden decrease at the beginning of the next highest manifold. Unfortunately, Sabo *et al.* do not present any results for the torsional wave functions of the $\pm 2^2$ levels. If the $\pm 2^2$ level can be interpreted as consisting of the τ_1 and τ_2 torsional normal modes, it is possible to look at the wave functions of these two individual levels and interpret the $\pm 2^2$ level as the product of the two. The results show that most of the probability is located close to the minimum structure and not in structures with deuterons in the plane. Therefore it appears that the $\pm 2^2$ level should not have a dramatically smaller inertial defect than other torsional levels, nor a negative ΔC value. On the other hand the observed small value of *B* and the change in inertial defect are rather easy to explain for the degenerate hydrogen bond stretch or a mixed stretch/torsional motion. A hydrogen bond stretching motion should generate a small positive change in the inertial defect, which together with a small torsional contribution, would explain the observed small negative change of the inertial defect.

The Coriolis constants ζ and $|\mu_{++}|$ of the 142.8 cm^{-1} band are similar to those of the $\pm 1^0$, and especially the $\pm 2^0$ levels. The $\pm 2^1$ level already has a negligible ζ so we expect a similar value for the higher $\pm 2^2$ level, although this is not certain. It is expected that the degenerate asymmetric stretch generates vibrational angular momentum, and all degenerate torsional levels appear to have a sizeable $|\mu_{++}|$ (see Table IV). The observed values of ζ and $|\mu_{++}|$ can then be explained by a combination band, with a $|\mu_{++}|$ value close to that of the $\pm 2^0$ level and that of ζ including contributions from both the asymmetric stretch and the $\pm 2^0$ level. Alternatively, the pure degenerate hydrogen bond stretch or a mixed level of the asymmetric stretch and torsion could still have an appreciable value of $|\mu_{++}|$ from the torsional motion and ζ from the asymmetric stretch. It was not possible to fit the respective contributions of the torsion and asymmetric stretch to ζ without correlation, in order to distinguish between the latter scenarios.

3. Bifurcation–tunneling splittings

The lack of observed bifurcation–tunneling splittings in the VRT spectrum is remarkable, and actually hindered the initial identification of the carrier of the band. The only evidence for a regular splitting due to bifurcation consists of the shoulders on the peaks, limiting the observed splittings to less than 1 MHz. Therefore the magnitude of the splitting for the excited state has to be about the same as for the ground state. The small tunneling splitting together with the anomalously large $K=0<-1$ splittings are difficult to rationalize with a purely torsional motion, but rather indicate a novel perturbation resulting from a new type of motion.

Generally, a significant increase of the bifurcation splitting with torsional energy has been observed, and from the previous results one would expect a splitting larger than 10 MHz—one order-of-magnitude larger than that observed. All of these previously observed level predominantly consist of the τ_1 torsional normal mode, whereas the $\pm 2^2$ level can be interpreted as a combination of the τ_1 and τ_2 normal modes. It is possible that the τ_2 normal mode does not couple to the bifurcation tunneling pathway, or couples to a different pathway containing an even number of flips of neighboring water molecules, perhaps with an opposite sign of the magnitude of the splitting. Therefore, we might then expect splittings of the same magnitude or even less than for the $\pm 1^0$ level (stemming mainly from the τ_1 contribution of the $\pm 1^0$ level). Although this speculative scenario could explain how the $\pm 2^2$ levels could lead to small regular bifurcation tunneling splitting, it fails to rationalize the large $K=0<-1$ splitting. van der Avoird *et al.*'s treatment of the torsional vibrations includes bifurcation tunneling and has explained the cause of the anomalous $K=0<-1$ splittings for the torsional states (see Fig. 5). Observation of an equal intensity triplet split by 10 MHz and caused by the mechanism found for the torsional states can only occur if the splitting is large ($\sim$15 MHz) and equal in ground and excited state. This is not the case, as van der Avoird *et al.* find an upper limit of 1.5 MHz for the magnitude of the splitting of the ground state.[36] Even taking the possible participation of the second bifurcation tunneling pathway (from the τ_2 mode) into account, the observation of a small regular splitting together with the splittings of the $K=0<-1$ transitions can therefore not be explained by the torsional vibrations.

The equal intensity triplet can be explained easily if the degenerate T_u- and T_g-levels are split but the A_g- and A_u-levels remain unaffected. This results in a 162:156:162 intensity ratio, which is identical with the observation, within the experimental uncertainty (see Fig. 3). From this analysis we conclude that the origin of this splitting is not from the same mechanism as in the previously observed torsional bands, strongly suggestive of a novel type of perturbation and new vibrational mode.

Excitation of the degenerate asymmetric stretch would be expected to only have a small effect on the regular bifurcation tunneling splittings through an insignificant weakening of the hydrogen bond, but no direct coupling to the bifurcation pathway. Although this does not explain the splittings of the $K=0<-1$ transitions, it is worth noting that for the degenerate asymmetric stretch, different pertur-

bations might exist than for the torsional levels.

In summary, the observed perturbations and successful utilization of the torsional Hamiltonian in the fit strongly suggest the presence of torsional motion in the vibration, but this could already arise from the torsional ground state of the molecule. The small intensity, values of the molecular constants (negative ΔB and ΔC, small change in inertial defect), and especially the extremely small bifurcation tunneling splitting together with the anomalously large splitting of the $K=0<-1$ transitions are only in agreement with assignment to a pure asymmetric stretching vibration or a mixed level or combination band of the degenerate asymmetric stretch with a torsional $\pm 2^n$ level.

V. DISCUSSION

The distinction between the four cases is important, as this determines whether the lowest excited purely translational level is at lower frequency. Sabo *et al*. predict that this should be the case through formation of a second pseudorotational manifold by the degenerate asymmetric stretch vibration.[21,22] As mentioned previously this could also produce mixed levels between any of the excited manifold states of the torsional and degenerate asymmetric stretch levels, essentially removing the distinction between torsional and translational levels.

Given the new information presented here, we can predict other bands in the vicinity which might enable the distinction between a purely torsional or translational vibration, a mixed level, or a combination band (see Fig. 6). In all cases, we can predict a parallel band at 134.3 cm^{-1} between the torsional $\pm 1^0$ level and the excited state of the 142.8 cm^{-1} band, regardless of its origin. This spectral region has not yet been studied, and in addition, such a study will be impeded by the small intensity for this transition, as it corresponds to a hot band. For a combination band of asymmetric stretch and the $\pm 2^0$ level, the asymmetric stretch fundamental itself then is predicted at 114.8 cm^{-1}, a region that similarly has not been investigated, but this frequency could also be shifted due to the coupling. If the degenerate asymmetric stretch gives rise to a pseudorotational manifold and we are observing a mixed level, predictions become difficult. In addition to the band at 134 cm^{-1} we would expect transitions to other levels of the stretching/torsional manifold resembling the 142.8 cm^{-1} band. For the case of a pure asymmetric stretch vibration with weak coupling to torsions and no formation of a pseudorotational manifold only the next highest torsional $k=\pm 2$ level should be observed. We shall proceed with a search of both the 134 and 114 cm^{-1} regions, as this should allow unambiguous vibrational assignment of the new band. Furthermore a search at higher frequencies for the purely torsional $\pm 2^2$ level or additional mixed levels will be undertaken. Last, a complete analysis of the anomalous splittings of the $K=0<-1$ transitions could be very useful in unambiguously assigning the 142.8 cm^{-1} band and confirming this as the first observation of a translational vibration for a water cluster.

Previous THz-VRT results for small water clusters have been used to test results calculated using intermolecular potential surfaces (IPS) and *ab initio* theory. This has been largely motivated by the quest for an accurate intermolecular potential for describing the liquid. Although the torsional degrees of freedom studied previously for the water trimer have allowed refinement of existing intermolecular potentials, inclusion of the translational motions presented here represents a qualitative advance for testing and developing such potentials.

The most straightforward test of any model potential is a comparison of the calculated and experimental structures. The structures calculated with potentials that were obtained by fitting to bulk properties of the liquid generally do not reproduce the experimentally observed cluster structures. Both *ab initio* calculations and potentials based on them generally predict these structures fairly well, but *ab initio* calculations themselves are only feasible for small systems.[3] Accurate potentials should attempt to also reproduce the vibrational energy levels and hydrogen bond tunneling dynamics of water clusters, as these are a very sensitive probe of the detailed surface topology, and not just the minima. Although both *ab initio* results and the potentials based on them reproduce the minimum energy structures quite well, they do not reproduce experimental vibrational frequencies, and the tunneling splittings calculated with intermolecular potentials are often inaccurate by orders-of-magnitude. By comparison VRT(ASP-W) and SAPT-5*s*-tuned do reproduce the tunneling splittings of the water dimer accurately, since they were fit to these data.[12,19]

TABLE VI. Comparison of the lowest calculated and experimental vibrational frequencies in cm^{-1} shows that the harmonic frequencies calculated by Xantheas and Klopper are significantly too large as the trimer exhibits extensive large amplitude torsional motions. The calculated frequencies for the asymmetric stretch are ~20% larger than the 142.8 cm^{-1} band.

Experiment[a]	Xantheas[b]	Klopper[c]
8.5 (torsion)	158	156.6 (torsion)
28.0 (torsion)	173	166.9 (*as*-stretch)
41.1 (torsion)	185	172.8 (as-stretch)
90.3 (torsion)	193	175.8 (torsion)
98.0 (torsion)	218	192.8 (torsion)
142.8 (*as*-stretch/torsion)[d]	235	207.5 (*s*-stretch)

[a]From Viant *et al.* (Ref. 26).
[b]Calculated by Xantheas *et al.* (Ref. 3).
[c]Results by Klopper *et al.* (Ref. 5).
[d]Reported here.

Table VI shows a comparison of some experimental vibrational frequencies for the water trimer and *ab initio* frequencies calculated using a harmonic approximation. Such calculations cannot reliably predict vibrational frequencies, as the water trimer is a weakly bound system and is very anharmonic. The 142.8 cm^{-1} band demonstrates this even for the stretching vibrations, which are expected to be less anharmonic than torsional vibrations. The lowest calculated *ab initio* torsional vibrational energy level is 142 cm^{-1} above the ground state, whereas experimentally nine levels, all due to one torsional vibration, have been found for $(D_2O)_3$ below 100 cm^{-1}. None of these calculations takes the correct symmetry of the ground state of the molecule into account, and for example, the calculations by Klopper and Xantheas both

give three different stretching vibrations. Calculations of cluster vibrations therefore must go beyond harmonic approximations and take coupling of various intermolecular degrees of freedom into account.[28]

Neglecting the intramolecular vibrational degrees of freedom a complete treatment of the IPS of the water trimer requires use of a 12D IPS. Fully coupled calculations for the trimer, utilizing IPS fit to *ab initio* or experimental results have not yet been possible, but instead a number of increasingly sophisticated models have been developed for the trimer, from early 1D torsional treatments up to the $(3+1)$D (torsions+symmetric stretch) treatment of Bacic *et al.* and the inclusion of torsion, overall rotation, and bifurcation tunneling by van der Avoird *et al.*[21,25,26,36] It has been predicted that the adiabatic separation of the torsional degrees of freedom from the translational and librational ones is fairly good, and Klopper has shown that the stretching vibrations appear to vary only slightly between different stationary points on the torsional potential energy surface.[5] Although the low lying torsional transitions of the water trimer appeared to vindicate this, Bacic *et al.* have recently shown that inclusion of the symmetric stretch is necessary to reproduce the experimentally observed rotational constants even for the first manifold of torsional energy levels.[21] He predicts that the higher torsional energy levels have to include coupling to all stretching vibrational degrees of freedom. The experimental observation of a stretch level with significant torsional motion appears to confirm that extensive coupling of the asymmetric stretch vibration with the torsional vibrations exists. We conclude that calculations attempting to reproduce experimental results at higher energies will require inclusion of both torsional and translational degrees of freedom as well as bifurcation tunneling and overall rotation. Unfortunately no calculations at a 6D level including all torsional and translational degrees of freedom exist, but these should now be feasible.

VI. CONCLUSIONS

We have reported the measurement of a vibrational band of $(D_2O)_3$ centered at 142.8 cm^{-1} in the translational band region of liquid water. Analysis shows that the band arises from transitions between the vibrational ground state and either the pure degenerate asymmetric stretch, or a combination band or mixed level of the asymmetric stretch and torsion. The band shows distinctly different tunneling splittings, unusual changes of the molecular constants for the excited state, as well as a much lower intensity than all previously recorded $(D_2O)_3$ bands, in support of this assignment.

This represents the first experimental observation of the hydrogen-bond stretching vibration for a water cluster by high resolution spectroscopy and allows comparison with theoretical calculations for this important class of motions in the liquid. Our analysis shows that calculations require explicit consideration of torsional and translational degrees of freedom, as they otherwise do not represent the true symmetric vibrational ground state structure, nor are able to take the observed coupling between the degenerate asymmetric stretch and torsional energy levels into account. Theoretical calculations taking all six torsional and stretching degrees of freedom into account are necessary to obtain a proper description of the energy levels in this frequency region.

ACKNOWLEDGMENT

This work was supported by the Experimental Physical Chemistry Program of the National Science Foundation.

[1] S. Suzuki and G. A. Blake, Chem. Phys. Lett. **229**, 499 (1994).
[2] D. J. Wales, J. Am. Chem. Soc. **115**, 11180 (1993).
[3] S. S. Xantheas and T. H. Dunning, Jr., J. Chem. Phys. **99**, 8774 (1993).
[4] W. Klopper and M. Schütz, Ber. Bunsenges. Phys. Chem. **99**, 469 (1995).
[5] W. Klopper, M. Schütz, H. P. Lüthi, and S. Leutwyler, J. Chem. Phys. **103**, 1085 (1995).
[6] W. Klopper and M. Schütz, Chem. Phys. Lett. **237**, 536 (1995).
[7] J. D. Cruzan, M. G. Brown, K. Liu, L. B. Braly, and R. J. Saykally, J. Chem. Phys. **105**, 6634 (1996).
[8] D. Sabo, Z. Bacic, T. Bürgi, and S. Leutwyler, Chem. Phys. Lett. **244**, 283 (1995).
[9] K. Liu, J. D. Cruzan, and R. J. Saykally, Science **271**, 929 (1996).
[10] K. Liu, M. G. Brown, J. D. Cruzan, and R. J. Saykally, J. Phys. Chem. A **101**, 9011 (1997).
[11] K. Liu, M. G. Brown, and R. J. Saykally, J. Phys. Chem. A **101**, 8995 (1997).
[12] R. S. Fellers, C. Leforestier, L. B. Braly, and M. G. Brown, Science **284**, 945 (1999).
[13] T. R. Dyke and J. S. Muenter, J. Chem. Phys. **60**, 2929 (1974).
[14] M. G. Brown, F. N. Keutsch, and R. J. Saykally, J. Chem. Phys. **109**, 9645 (1998).
[15] J. B. Paul, R. A. Provencal, and R. J. Saykally, J. Phys. Chem. A **102**, 3279 (1998).
[16] M. G. Brown, F. N. Keutsch, L. B. Braly, and R. J. Saykally, J. Chem. Phys. **111**, 7801 (1999).
[17] L. B. Braly, J. D. Cruzan, K. Liu, R. S. Fellers, and R. J. Saykally, J. Chem. Phys. **112**, 10293 (2000).
[18] E. M. Mas and K. Szalewicz, J. Chem. Phys. **104**, 7606 (1996).
[19] G. C. Groenenboom, E. M. Mas, R. Bukowski, K. Szalewicz, P. E. S. Wormer, and A. van der Avoird, Phys. Rev. Lett. **84**, 4072 (2000).
[20] D. Sabo, Z. Bacic, S. Graf, and S. Leutwyler, Chem. Phys. Lett. **261**, 318 (1996).
[21] D. Sabo, Z. Bacic, S. Graf, and S. Leutwyler, J. Chem. Phys. **111**, 5331 (1999).
[22] D. Sabo, Z. Bacic, S. Graf, and Leutwyler, J. Chem. Phys. **110**, 5745 (1999).
[23] D. Sabo and Z. Bacic, J. Chem. Phys. **111**, 10727 (1999).
[24] D. J. Wales, J. Chem. Soc., Faraday Trans. **92**, 2505 (1996).
[25] A. van der Avoird, E. H. T. Olthof, and P. E. S. Wormer, J. Chem. Phys. **105**, 8034 (1996).
[26] M. R. Viant, M. G. Brown, J. D. Cruzan, R. J. Saykally, M. Geleijns, and A. van der Avoird, J. Chem. Phys. **110**, 4369 (1999).
[27] M. G. Brown, M. R. Viant, R. P. McLaughlin, C. J. Keoshian, E. Michael, J. D. Cruzan, R. J. Saykally, M. Geleijns, and A. van der Avoird, J. Chem. Phys. **111**, 7789 (1999).
[28] F. N. Keutsch, E. N. Karyakin, R. J. Saykally, and A. van der Avoird, J. Chem. Phys. **114**, 3988 (2001), preceding paper.
[29] F. N. Keutsch, R. Fellers, M. R. Viant, and R. J. Saykally, J. Chem. Phys. **114**, 4005 (2001), following paper.
[30] M. R. Viant, J. D. Cruzan, D. D. Lucas, M. G. Brown, K. Liu, and R. J. Saykally, J. Phys. Chem. A **101**, 9032 (1997).
[31] W. B. Bosma, L. E. Fried, and S. Mukamel, J. Chem. Phys. **98**, 4413 (1993).
[32] G. A. Blake, K. B. Laughlin, R. C. Cohen, K. L. Busarow, D. H. Gwo, C. A. Schmuttenmaer, D. W. Steyert, and R. J. Saykally, Rev. Sci. Instrum. **62**, 1693 (1991).
[33] G. A. Blake, K. B. Laughlin, R. C. Cohen, K. L. Busarow, D. H. Gwo, C. A. Schmuttenmaer, D. W. Steyert, and R. J. Saykally, Rev. Sci. Instrum. **62**, 1701 (1991).

[34] K. Liu, R. S. Fellers, M. R. Viant, R. P. McLaughlin, M. G. Brown, and R. J. Saykally, Rev. Sci. Instrum. **67**, 410 (1996).
[35] W. L. Bishop, S. M. Marazita, P. A. D. Wood, and T. W. Crowe, Seventh International Symposium on Space Terahertz Technology, Charlottesville, 1996.
[36] E. H. T. Olthof, A. van der Avoird, P. E. S. Wormer, K. Liu, and R. J. Saykally, J. Chem. Phys. **105**, 8051 (1996).
[37] M. Geleijns (private communication).
[38] M. Geleijns and A. van der Avoird, J. Chem. Phys. **110**, 823 (1999).
[39] N. Pugliano and R. J. Saykally, Science **257**, 1937 (1992).